A Heat-Balance Model with a Canopy of One or Two Layers and its Application to Field Experiments

著者	Yamazaki Takeshi, Kondo Junsei, Watanabe Tsutomu, Sato Takeshi
journal or publication title	Journal of Applied Meteorology
volume	31
number	1
page range	86-103
year	1992
URL	http://hdl.handle.net/10097/51862

doi: 10.1175/1520-0450(1992)031<0086:AHBMWA>2.0.CO;2

A Heat-Balance Model with a Canopy of One or Two Layers and its Application to Field Experiments

TAKESHI YAMAZAKI, JUNSEI KONDO, AND TSUTOMU WATANABE

Geophysical Institute, Tohoku University, Sendai, Japan

TAKESHI SATO

Shinjo Branch of Snow and Ice Studies, National Research Institute for Earth Science and Disaster Prevention, Shinjo, Japan

(Manuscript received 12 November 1990, in final form 22 April 1991)

ABSTRACT

A heat-balance model having a canopy of one or two layers has been developed. The calculated fluxes using the present model were found to be in agreement with measurements from a rice paddy field, an orchard, and the calculated fluxes of a multilayer model. Although there was some difference in the calculated fluxes between the one- and two-layer models, the one-layer model was found to be sufficient when the dependency of the radiative ground-surface temperature on the viewing angle was not considered.

1. Introduction

In the present study, a simple heat-balance model with one or two canopy layers is developed. One of the purposes of the model is to estimate the same sensible and latent heat fluxes between a vegetated surface and the atmosphere in the steady states as those calculated with more realistic multilayer models. In fact, a comparison will be made of results between the one- or two-layer model and a multilayer model, which has the same physical processes or parameterizations as the present model. This simple canopy model can easily predict the dependence of the heat balance on various parameters. It is suitable to combine with atmospheric, soil layer, and/or snow-cover models. For example, the model can be coupled with a heat-balance snowmelt model (Kondo and Yamazaki 1990) and applied to a forested region with snow cover.

Kondo and Akashi (1976) produced a multilayer model and a guideline for the parameterization of the flow in and above canopy layers, while Kondo and Kawanaka (1986) extended it to calculate the sensible heat exchange. Kondo and Watanabe (1992) further developed this model to incorporate latent heat exchange. These models can calculate some profiles in the canopy; however, they require much computing time. Models with more realistic detail have been developed for use in general circulation models (e.g., Dickinson 1984; Sellers et al. 1986). These models involve many vegetation parameters that are, in practicality, difficult to determine. From this point of view, simple models with several canopy layers are preferable. Deardorff (1978) has suggested a one-canopy-layer model. Recently, models with two canopy layers have also been proposed (van de Griend and Boxel 1989). However, it has not been sufficiently discussed whether one, two, or more layers are necessary to accurately estimate the energy exchange.

In this paper models having one and two canopy layers are developed. Each model is capable of estimating almost the same fluxes as those calculated with the multilayer model described by Kondo and Watanabe (1992, hereafter MLM).

Section 2 of the present paper describes the two-layer model in detail, while section 3 describes the one-layer model. In section 4, the observed values of the heat balance of a rice paddy field and an orchard are compared with the model calculations. Section 5 describes the differences among the one-layer, two-layer, and MLM models. Section 6 discusses two problems associated with the use of the two-layer model: the nonequilibrium problem of the soil layer, and the dependency of radiative ground temperature on the viewing angle.

2. Two-layer model (2LM)

a. The heat balance in the 2LM

Figure 1 shows the schematic representation of the two-layer model (henceforth 2LM); the symbols used are listed in the Appendix. The canopy is divided into a "crown space" and "trunk space" (without leaves), while the crown space is further divided into a lower

Corresponding author address: Takeshi Yamazaki, Geophysical Institute, Tohoku University, Sendai 980, Japan.

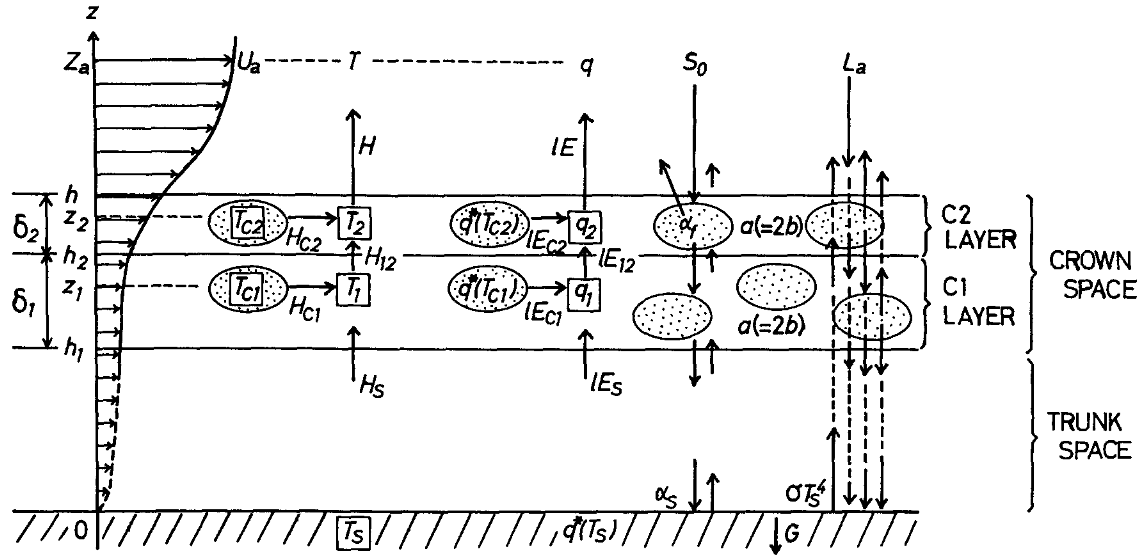

FIG. 1. Schematic diagram of the two-layer model (2LM). Symbols are listed in the Appendix.

layer ($C1$) and an upper layer ($C2$). The tendency of temperature distribution is obtained by this division (see section 2g for how to divide). The heat balance is solved with respect to the radiative, sensible, and latent heat fluxes among the atmosphere, the two crown layers, and soil surface. In the present study, heat storage within canopy elements and heat associated with photosynthesis are neglected, and, for simplification, the leaf-area densities of each layer are assumed to be equal.

The heat-balance equations for each layer are as follows:

lower canopy layer ($C1$ layer),

$$S_{n1} + L_{n1} = H_{C1} + lE_{C1}; \qquad (1)$$

upper canopy layer ($C2$ layer),

$$S_{n2} + L_{n2} = H_{C2} + lE_{C2}; \qquad (2)$$

soil surface,

$$S_{nS} + L_{nS} = H_S + lE_S + G. \qquad (3)$$

Here S_{ni} and L_{ni} ($i = 1, 2, S$) are the net absorption of solar and infrared radiation (section 2b), H_{Ci} and lE_{Ci} the sensible and latent heat fluxes from the canopy elements to the surrounding air in the ith layer, H_S and lE_S the sensible and latent heat from the soil surface to trunk space (section 2c), and G the heat flux into the soil layer. Although G in the present model is given as an external condition, it can be a variable predicted with use of an appropriate soil-layer model (e.g., solving heat conduction equations, force–restore method, and other parameterizations of G).

The flux H_{C1} is equal to the difference between the upward sensible heat flux (H_{12}) at the top of the $C1$ layer and that (H_S) at the bottom of the $C1$ layer; that is,

$$H_{C1} = H_{12} - H_S. \qquad (4)$$

In the same manner as H_{C1},

$$H_{C2} = H - H_{12}, \qquad (5)$$

where H is the sensible heat flux from the top of the canopy layer to the atmosphere. For latent heat fluxes,

$$lE_{C1} = lE_{12} - lE_S \qquad (6)$$

and

$$lE_{C2} = lE - lE_{12}. \qquad (7)$$

Note that the fluxes H_S and lE_S are the same as those at the soil surface, since there are no canopy elements in the trunk space.

In the following subsections, each term in Eqs. (1)–(7) will be described with canopy parameters (canopy height, leaf-area density, etc.), external conditions (meteorological conditions above the canopy), and unknown variables such as leaf surface temperatures, T_{C1}, T_{C2}, soil surface temperature T_S, air temperature, and specific humidity in each canopy layer T_1, T_2, q_1, and q_2. Since there are seven equations for the seven unknown variables, these equations can be easily solved to obtain heat-balance terms (section 2i).

b. Radiation

Leaves are considered as blackbodies for short- and longwave radiation. At the canopy top, however, the reflectance of individual leaves is replaced by α_f in order to take into account the reflection of solar radiation by the canopy. It is assumed that the soil surface has an emissivity equal to unity and its reflectance of solar radiation α_S is isotropic.

1) Solar radiation

The individual terms associated with solar radiation are written as

$$S_{n1} = S^{\downarrow}(h_2) - S^{\downarrow}(h_1) + S^{\uparrow}(h_1) - S^{\uparrow}(h_2), \quad (8)$$

$$S_{n2} = (1 - \alpha_f')S_0 - S^{\downarrow}(h_2) + S^{\uparrow}(h_2) - S^{\uparrow}(h), \quad (9)$$

and

$$S_{nS} = S^{\downarrow}(h_1) - S^{\uparrow}(h_1), \quad (10)$$

where $S^{\downarrow}(z)$ and $S^{\uparrow}(z)$ are the downward and upward solar radiation fluxes through a horizontal plane at the height z, respectively, and can be written as follows:

$$S^{\downarrow}(h_2) = (1 - \alpha_f')X_{m2}S_0,$$

$$S^{\downarrow}(h_1) = X_{m1}S^{\downarrow}(h_2) = (1 - \alpha_f')X_{m1}X_{m2}S_0,$$

$$S^{\uparrow}(h_1) = \alpha_S S^{\downarrow}(h_1) = (1 - \alpha_f')\alpha_S X_{m1}X_{m2}S_0,$$

$$S^{\uparrow}(h_2) = X_1 S^{\uparrow}(h_1) = (1 - \alpha_f')\alpha_S X_{m1}X_{m2}X_1 S_0,$$

$$S^{\uparrow}(h) = X_2 S^{\uparrow}(h_2) = (1 - \alpha_f')\alpha_S X_{m1}X_{m2}X_1 X_2 S_0,$$

with

$$\alpha_f' \equiv (1 - X_{m1}X_{m2})\alpha_f.$$

Here S_0 is the incoming solar radiation at the top of the canopy, while α_f' is the albedo for the entire canopy when $\alpha_S = 0$. The variables X_{mi} and X_i $(i = 1, 2)$ are the transmittance of the Ci layer for the direct solar beam and the reflected radiation, respectively, which are given by

$$X_{mi} = \exp(-m\delta_i b), \quad (m = \sec\theta) \quad (11)$$

and

$$X_i = \exp(-1.66\delta_i b), \quad (i = 1, 2). \quad (12)$$

Here δ_i is the thickness of the Ci layer, θ the solar zenith angle, and b the attenuation coefficient for radiation. In this study, b is assumed to be $a/2$, which corresponds to a random distribution of leaf orientation (if the foliage has only horizontal leaves, $b = a$). The coefficient 1.66 is the *diffusivity factor*.

The albedo of the entire canopy α can be written as

$$\alpha = \frac{\alpha_f' S_0 + S^{\uparrow}(h)}{S_0}$$

$$= \alpha_f' + (1 - \alpha_f')\alpha_S X_{m1}X_{m2}X_1X_2$$

$$= (1 - X_{m1}X_{m2})\alpha_f + [1 - (1 - X_{m1}X_{m2})\alpha_f] \times \alpha_S X_{m1}X_{m2}X_1X_2. \quad (13)$$

The value of α converges to α_S when the canopy is very sparse, and to α_f when it is very dense. This value also varies diurnally with the solar zenith angle.

2) Infrared radiation

In the same manner as solar radiation, the infrared radiation terms can be written as

$$L_{n1} = L^{\downarrow}(h_2) - L^{\downarrow}(h_1) + L^{\uparrow}(h_1) - L^{\uparrow}(h_2), \quad (14)$$

$$L_{n2} = L_a - L^{\downarrow}(h_2) + L^{\uparrow}(h_2) - L^{\uparrow}(h), \quad (15)$$

and

$$L_{nS} = L^{\downarrow}(h_1) - L^{\uparrow}(h_1). \quad (16)$$

Here

$$L^{\downarrow}(h_2) = X_2 L_a + (1 - X_2)\sigma T_{C2}^4,$$

$$L^{\downarrow}(h_1) = X_1 L^{\downarrow}(h_2) + (1 - X_1)\sigma T_{C1}^4 = X_1X_2L_a + X_1(1 - X_2)\sigma T_{C2}^4 + (1 - X_1)\sigma T_{C1}^4,$$

$$L^{\uparrow}(h_1) = \sigma T_S^4,$$

$$L^{\uparrow}(h_2) = X_1 L^{\uparrow}(h_1) + (1 - X_1)\sigma T_{C1}^4 = X_1\sigma T_S^4 + (1 - X_1)\sigma T_{C1}^4,$$

and

$$L^{\uparrow}(h) = X_2 L^{\uparrow}(h_2) + (1 - X_2)\sigma T_{C2}^4 = X_1X_2\sigma T_S^4 + X_2(1 - X_1)\sigma T_{C1}^4 + (1 - X_2)\sigma T_{C2}^4.$$

In the above, L_a is the downward atmospheric radiation incident on the canopy, T_{Ci} the surface temperature of the leaves in the Ci layer, and T_S the soil surface temperature. The transmittance for infrared radiation X_i is the same as that for the reflected solar radiation [given by Eq. (12)].

c. *Sensible and latent heat fluxes*

1) Fluxes within the canopy

The sensible heat flux H_{Ci} from the canopy elements to the surrounding air in the Ci layer can be written as

$$H_{Ci} = C_P\rho c_h a\delta_i U(z_i)(T_{Ci} - T_i) = A_{Ci}(T_{Ci} - T_i), \quad (17)$$

where

$$A_{Ci} \equiv C_P\rho c_h a\delta_i U(z_i).$$

In the above, c_h is the heat transfer coefficient of individual leaves and T_i the air temperature in the Ci layer. Wind speed $U(z)$ will be described in section 2d, and z_i is the representative height of the Ci layer (section 2g). The sensible heat from the soil surface H_S is given by

$$H_S = C_P\rho C_{HS}U(h_1)(T_S - T_1) = A_S(T_S - T_1), \quad (18)$$

where

$$A_S \equiv C_P\rho C_{HS}U(h_1).$$

In Eq. (18) C_{HS} is the bulk transfer coefficient of sensible heat for the soil surface (the reference height is h_1).

For the latent heat flux,

$$lE_{Ci} = l\rho c_{ei} a\delta_i U(z_i)[q^*(T_{Ci}) - q_i]$$
$$= A_{Cie}[q^*(T_{Ci}) - q_i], \quad (19)$$

with

$$c_{ei} = j_i c_h \quad (0 \leqslant j_i \leqslant 1).$$

The variable j_i is the evapotranspiration factor of a leaf ($j_i = 1$ for completely wet foliage, $j_i = 0$ for dead foliage), which is controlled by plant physiology (see section 2h). Similarly,

$$lE_S = l\rho\beta_S C_{HS}U(h_1)[q^*(T_S) - q_1]$$
$$= A_{S1e}[q^*(T_S) - q_1], \quad (20)$$

where β_S is the soil-moisture availability, which is described, for example, by the soil-water content in the upper 2 cm of the soil (Kondo et al. 1990).

The flux H_{12} is given by

$$H_{12} = C_P\rho K_H(h_2)\frac{T_1 - T_2}{z_1 - z_2} = K'(T_1 - T_2), \quad (21)$$

defining K' as

$$K' \equiv \frac{C_P\rho K_H(h_2)}{z_1 - z_2}.$$

Here K_H is the eddy diffusivity for sensible heat transfer, and is written using mixing-length notation Λ as

$$K_H(z) = \Lambda^2(z)\frac{dU}{dz}. \quad (22)$$

Then $K_H(h_2)$ can be approximated as follows:

$$K_H(h_2) \approx \Lambda^2(h_2)\frac{U(z_1) - U(z_2)}{z_1 - z_2}. \quad (23)$$

See section 2e for a discussion of the mixing length.

The latent heat lE_{12} is written as

$$lE_{12} = l\rho K_E(h_2)\frac{q_1 - q_2}{z_1 - z_2} = K'_e(q_1 - q_2), \quad (24)$$

where

$$K'_e \equiv \frac{l\rho K_E(h_2)}{z_1 - z_2}.$$

Here K_E is the eddy diffusivity for vapor transfer and $K_E = K_H$ is assumed. Note that H and lE are not sensitive to K_E and K_H. For example, H and lE change by only a few watts per square meter for the change of factor 2 in K_E and K_H.

2) FLUXES FROM THE CANOPY TO THE ATMOSPHERE

When taking the atmospheric stability into account, the sensible heat flux from the canopy layer to the atmosphere H is written as

$$H = A_0(T_2 - T), \quad (25)$$

where

$$A_0 \equiv C_P\rho\frac{ku_*}{\Psi_h},$$

$$\Psi_h = \int_{\zeta_1}^{\zeta_2}\frac{\phi_h(\zeta)}{\zeta}d\zeta,$$

$$\zeta_1 = \frac{h - d}{L}, \quad \text{and} \quad \zeta_2 = \frac{z_a - d}{L}.$$

In the above, T is the air temperature at $z = z_a$ ($z_a > h$), k the von Kármán constant, u_* the friction velocity, d the zero-plane displacement, L the Monin–Obukhov length, and ϕ_h the nondimensional temperature gradient (Kondo 1975).

Similarly, the latent heat flux from the canopy to the atmosphere lE is written as

$$lE = A_{0e}(q_2 - q), \quad (26)$$

with

$$A_{0e} \equiv l\rho\frac{ku_*}{\Psi_e}.$$

Here $\Psi_e = \Psi_h$ is assumed.

d. Wind-speed profile

The wind-speed profile within the canopy can be obtained by solving the momentum diffusion equation; however, it is impossible to solve this equation analytically, due to its nonlinearity. Therefore, the wind profile is described by a simple function. Its functional form is determined according to the MLM, with a new mixing length (see section 2e).

Profiles of wind speed depend on the nondimensional canopy density, defined by

$$c_* = c_d a h, \quad (27)$$

where c_d is the drag coefficient of individual leaves, a the leaf-area density (one-sided area per unit volume), and h the canopy height.

The wind profile should satisfy the following conditions.

(i) If $c_* \to 0$, the wind profile converges to the logarithmic profile,

$$U(z) = U(h)\frac{\ln(z/z_{0S})}{\ln(h/z_{0S})}, \qquad (28)$$

where z_{0S} is the roughness length for the soil surface underneath the canopy.

(ii) For large c_*, the wind coincides with the exponential profile (e.g., see Inoue 1963):

$$U(z) = U(h)\exp\left[-\frac{c_*}{2k^2}\left(1-\frac{z}{h}\right)\right], \qquad (29)$$

where k is the von Kármán constant.

(iii) It varies smoothly with c_*.

To satisfy these conditions, the wind speed can be expressed by the sum of the logarithmic term and exponential term:

$$\frac{U(z)}{U(h)} = f\exp\left[-\frac{c_{*1}}{2k^2}\left(1-\frac{z}{h}\right)\right] + (1-f)\frac{\ln(z/z_{0S})}{\ln(h/z_{0S})}, \qquad (30)$$

where f is a weighting function for c_*. The wind speed near the ground ($z \rightarrow 0$) calculated by Eq. (29) does not decrease very well when c_* decreases. To improve this, a modified canopy density c_{*1} is introduced, which is determined so the wind speed profile coincides with that calculated by the MLM.

When leaves exist only between $h/2$ and h with a constant density, the results can be written as

$$f = \frac{0.494(x+0.8)}{[(x+0.8)(x-0.5)+1.1]^{1/2}} + 0.37, \qquad (-3 \leqslant x \leqslant 1), \qquad (31)$$

$$x \equiv \log c_*,$$

$$\log c_{*1} = \frac{(x+0.26)+[(x+0.26)^2+0.16]^{1/2}}{2} - 0.3, \qquad (-3 \leqslant x \leqslant 1). \qquad (32)$$

The dependences of f and c_{*1} on the canopy density

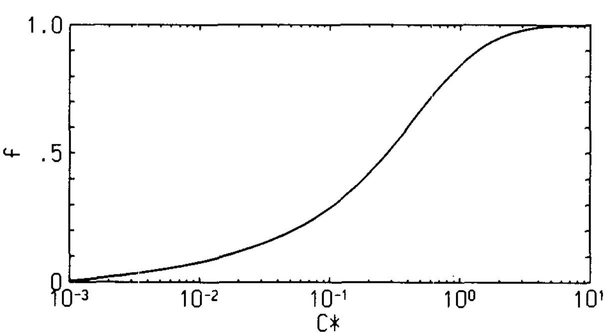

FIG. 2. The weighting function for the wind profile f as a function of the nondimensional canopy density.

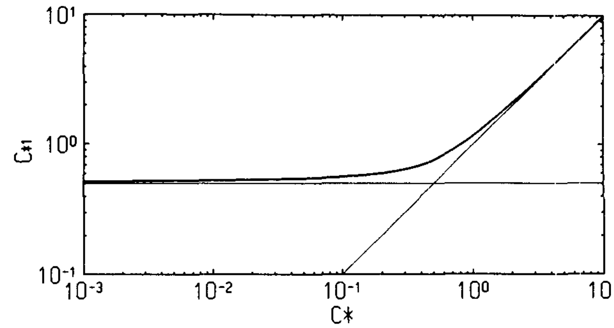

FIG. 3. The modified canopy density for wind profile c_{*1} as a function of the nondimensional canopy density.

c_* are shown in Figs. 2 and 3, respectively. Wind profile examples for various values of c_* are shown in Fig. 4. While the wind profiles based on Eq. (30) are not smooth at $z = h_1$ for medium values of c_*, the wind speeds agree with the MLM results within an error of 0.05 m s^{-1} for $U_a = 5$ m s^{-1}.

The wind profile above the canopy is given by

$$U = \frac{u_*}{k}\Psi_m,$$

$$\Psi_m = \int_{\zeta_0}^{\zeta_z}\frac{\phi_m(\zeta)}{\zeta}d\zeta, \qquad (33)$$

with

$$\zeta_z = \frac{z-d}{L}, \quad \zeta_0 = \frac{z_0}{L}, \quad z \geqslant h.$$

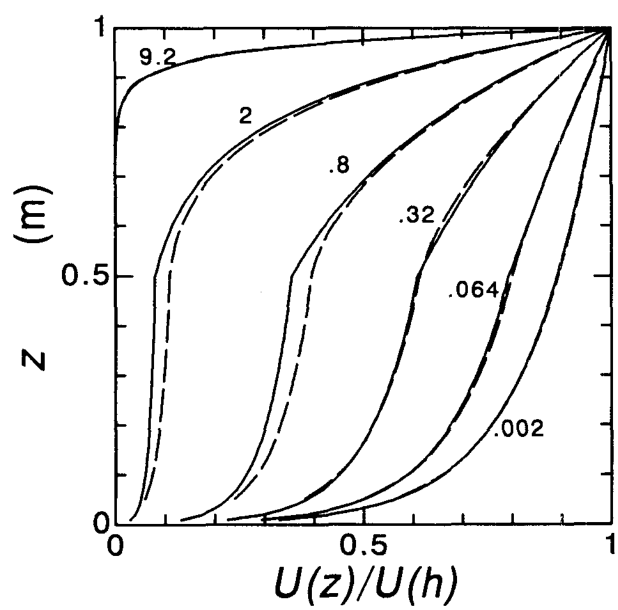

FIG. 4. Examples of wind profiles calculated by Eq. (30) for $h = 1$ m and $h_1 = 0.5$ m. Solid lines: present model [Eq. (30)]. Broken lines: MLM.

Here ϕ_m is the nondimensional wind shear (Kondo 1975).

Within the trunk space ($z < h_1$), the logarithmic wind profile is assumed; that is,

$$U = \frac{u_{*s}}{k} \ln \frac{z}{z_{0S}}, \quad z < h_1, \tag{34}$$

where u_{*s} and z_{0S} are the friction velocity in the trunk space and the roughness length for the soil surface below the canopy, respectively. The so-called secondary wind-speed maximum, which is observed in some cases for a trunk space with a dense canopy, cannot be described in this model. However, such a maximum does not influence the heat balance, since the wind is weak in dense canopies.

e. Mixing length

According to Watanabe and Kondo (1990), the mixing length for the canopy Λ is written as

$$\Lambda(z) = k \int_0^z \left\{ r \exp\left[-\int_0^r \mu(z-t)dt \right] \mu(z-r) \right\} dr + kz \exp\left[-\int_0^z \mu(z-t)dt \right], \tag{35}$$

where

$$\mu(z) = \frac{c_d a(z)}{2k^2}.$$

Note that Eq. (35) should be modified for large values of $|da(z)/dz|$ (see Watanabe and Kondo 1990). If the leaf-area density is constant with height, Λ in the upper part of crown space can be written as

$$\Lambda(z) = kh \left\{ \left(\frac{h_1}{h} - \frac{2k^2}{c_*} \right) \times \exp\left[-\frac{c_*}{2k^2 h}(z - h_1) \right] + \frac{2k^2}{c_*} \right\}, \tag{36}$$

where h_1 is the bottom of the crown space. The value of $\Lambda(h_2)$ shown in Eq. (23) was calculated using (36).

At the top of the canopy ($z = h$), the expression can be rewritten as

$$\frac{\Lambda(h)}{h} = k \left\{ \left(\frac{h_1}{h} - \frac{2k^2}{c_*} \right) \times \exp\left[-\frac{c_*}{2k^2}\left(1 - \frac{h_1}{h}\right) \right] + \frac{2k^2}{c_*} \right\}. \tag{37}$$

Note that the right-hand side of (37) reduces to k for $c_* \to 0$. Thus, $\Lambda(h)/h$ depends on c_* and h_1/h. On the other hand, above the canopy,

$$\Lambda(z) = k(z - d), \quad z \geq h. \tag{38}$$

which yields a logarithmic wind profile.

f. Zero-plane displacement and roughness length

The zero-plane displacement and the roughness length are related to the density of the canopy. When considering the continuity of Λ at the top of the canopy ($z = h$), the following expression can be obtained from Eqs. (37) and (38):

$$\frac{d}{h} = 1 - \frac{\Lambda(h)}{kh} = 1 - \left(\frac{h_1}{h} - \frac{2k^2}{c_*} \right) \times \exp\left[-\frac{c_*}{2k^2}\left(1 - \frac{h_1}{h}\right) \right] - \frac{2k^2}{c_*}. \tag{39}$$

For this case, since the purpose is to connect the wind profile at $z = h$ (not considered above the canopy), neutral conditions are assumed for simplicity. Therefore, the friction velocity u_* at the top of the canopy ($z = h$) is given as

$$\frac{u_*}{U(h)} = k \left(\ln \frac{h-d}{z_0} \right)^{-1}. \tag{40}$$

On the other hand, from the definition of Λ, u_* is written in terms of the mixing length

$$u_* = \Lambda(h) \left. \frac{\partial U}{\partial z} \right|_{z=h}. \tag{41}$$

Substitution of Eq. (38) and the derivative of (30) into (41) yields

$$\frac{u_*}{U(h)} = k \left(1 - \frac{d}{h} \right) \left[f \frac{c_{*1}}{2k^2} + \frac{1-f}{\ln(h/z_{0S})} \right]. \tag{42}$$

From Eqs. (40) and (42), the following relationship is obtained:

$$\frac{z_0}{h} = \left(1 - \frac{d}{h}\right) \exp\left\langle -\left\{ \left(1 - \frac{d}{h}\right) \times \left[f \frac{c_{*1}}{2k^2} + \frac{1-f}{\ln(h/z_{0S})} \right] \right\}^{-1} \right\rangle. \tag{43}$$

Equation (43), with (31), (32), and (39), yields the value of z_0/h for any c_* and h_1/h.

The dependencies of d and z_0 on the canopy density c_* are shown in Figs. 5 and 6, respectively. The upper scales of these figures are the value of c_* divided by $2k^2$ (=0.32). Canopies can be roughly classified into sparse and dense canopies at $c_*/2k^2 = 1$.

g. Division into two layers

The following formulation was verified by comparing the fluxes H and lE with the fluxes from the MLM. The boundary between the two layers within the crown space h_2 is given by

$$h_2 = \max(h_{21}, h_{22}),$$
$$h_{21} = h - 1.6(h - d),$$
$$h_{22} = \frac{h_1 + h}{2}, \tag{44}$$

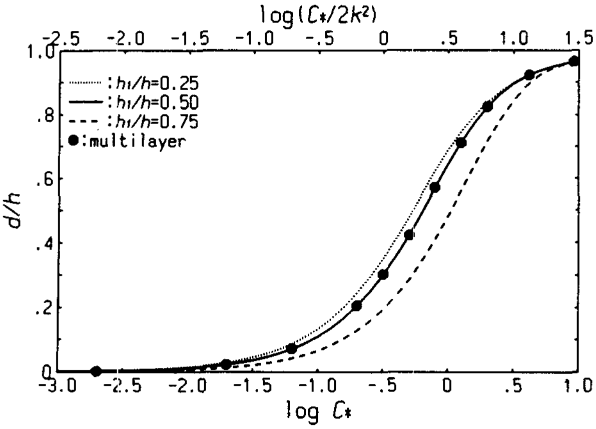

FIG. 5. The relation between the zero-plane displacement and canopy density for various values of h_1/h. Points are calculated with the MLM for $h_1/h = 0.5$.

where h_{21} is an intermediate height where the wind speed is approximately one-fifth that at the top of a dense canopy ($\ln 5 \approx 1.6$), and h_{22} is just the geometrical mean height. For a dense canopy, $h_2 = h_{21}$ because $h_{21} > h_{22}$, and h_2 increases as the density of the canopy increases. Since most of the momentum is absorbed and the exchange of energy is active at the top layer of a dense canopy, the C2 layer should be thinner.

The representative heights for the wind speed z_1 and z_2 are assumed as follows. For a sparse canopy ($f < 0.5$), since the wind-speed difference between top and bottom is small, the representative height is chosen as middle of each layer:

$$z_1 = \frac{h_2 + h_1}{2}, \quad f < 0.5, \tag{45}$$

and

$$z_2 = \frac{h + h_2}{2}, \quad f < 0.5. \tag{46}$$

For a dense canopy ($f \geqslant 0.5$):

$$\exp[-\mu_0(h - z_1)] = \frac{1}{\delta_1} \int_{h_1}^{h_2} \exp[-\mu_0(h - z)]dz, \tag{47}$$

and

$$\exp[-\mu_0(h - z_2)] = \frac{1}{\delta_2} \int_{h_2}^{h} \exp[-\mu_0(h - z)]dz, \tag{48}$$

where

$$\mu_0 = \frac{c_d a}{2k^2} = \frac{c_*}{2k^2 h}.$$

The variables z_1 and z_2 in Eqs. (47) and (48) are the heights where the mean wind speed of each layer is found, which can be written using (29) as

$$z_1 = \frac{1}{\mu_0} \ln \frac{\exp(\mu_0 h_2) - \exp(\mu_0 h_1)}{\delta_1 \mu_0}, \quad f \geqslant 0.5 \tag{49}$$

and

$$z_2 = \frac{1}{\mu_0} \ln \frac{\exp(\mu_0 h) - \exp(\mu_0 h_2)}{\delta_2 \mu_0}, \quad f \geqslant 0.5. \tag{50}$$

h. Evapotranspiration factor of a leaf

In order to make canopy models realistic, appropriate values of the transfer coefficients of individual leaves c_d, c_h, and c_e are required. While they are dependent on the size and shape of the canopy elements, c_e also depends on the physiology of the plant. Many studies have been made on the stomatal resistance associated with transpiration. The relationships between the resistances and the transfer coefficients in this paper are written as

$$c_h U = r_a^{-1}, \tag{51}$$

$$c_e U = (r_a + r_s)^{-1}, \tag{52}$$

where r_a is the aerodynamic resistance of the leaf surface and r_s the stomatal resistance. Thus, the evapotranspiration factor of a leaf j is written as

$$j = \frac{c_e}{c_h} = \frac{1}{1 + c_h U r_s}. \tag{53}$$

Inoue et al. (1984) experimentally obtained r_s as

$$r_s = r_m(1 + S_{\rm abm}/S_{\rm ab})\Omega, \tag{54}$$

where $S_{\rm ab}$ is the shortwave radiation absorbed by a unit of leaf area, r_m the minimum value of r_s, $S_{\rm abm}$ the value of $S_{\rm ab}$ when $r_s = 2r_m$, and Ω a factor expressing the influence of humidity and air temperature upon r_s. Substituting Eq. (54) into (53), j can be written as

$$j = \frac{1}{1 + c_h U r_m(1 + S_{\rm abm}/S_{\rm ab})\Omega}. \tag{55}$$

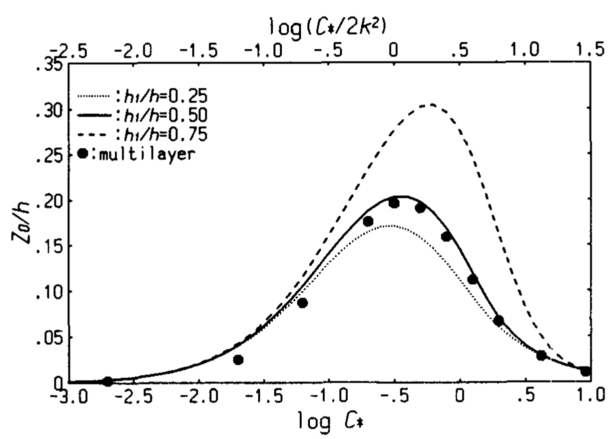

FIG. 6. The relation between the roughness length and canopy density for various values of h_1/h. Points are calculated with the MLM for $h_1/h = 0.5$.

In the 2LM, j_i is calculated for each layer using $U(z_i)$ and S_{abi}, where S_{abi} is the value of S_{ab} for the Ci layer, given by

$$S_{abi} = S_{ni}(a\delta_i)^{-1}, \quad (i = 1, 2). \tag{56}$$

i. Implementing the model

The fourth power of temperature and saturation specific humidity can be approximated as follows:

$$T_{Ci}^4 \approx T^4 + 4T^3(T_{Ci} - T), \quad (i = 1, 2), \tag{57}$$

$$T_S^4 \approx T^4 + 4T^3(T_S - T), \tag{58}$$

$$q^*(T_{Ci}) \approx q^*(T_{Ci\text{old}}) + \Delta_i(T_{Ci} - T_{Ci\text{old}}), \tag{59}$$

$$q^*(T_S) \approx q^*(T_{S\text{old}}) + \Delta_S(T_S - T_{S\text{old}}), \tag{60}$$

where

$$\Delta_i = \frac{dq^*(T_{Ci\text{old}})}{dT}, \quad \text{and} \quad \Delta_S = \frac{dq^*(T_{S\text{old}})}{dT}.$$

Equations (1)–(7) become simultaneous simple equations for seven unknown variables, T_1, T_2, T_S, T_{C1}, T_{C2}, q_1, and q_2. The suffix "old" denotes the value whose degree of approximation is lower by one step. Consequently, the following set of simultaneous equations is obtained:

$$\begin{bmatrix} A_{C1} & 0 & (1-X_1)Y & Y_1 & (1-X_1)(1-X_2)Y & A_{C1e} & 0 \\ 0 & A_{C2} & X_1(1-X_2)Y & (1-X_1)(1-X_2)Y & Y_2 & 0 & A_{C2e} \\ A_S & 0 & -Y - A_S - A_{S1e}\Delta_S & (1-X_1)Y & X_1(1-X_2)Y & A_{S1e} & 0 \\ -A_{C1} - K' - A_S & K' & A_S & A_{C1} & 0 & 0 & 0 \\ K' & -A_{C2} - A_0 - K' & 0 & 0 & A_{C2} & 0 & 0 \\ 0 & 0 & A_{S1e}\Delta_S & A_{C1e}\Delta_1 & 0 & -A_{C1e} - K'_e - A_{S1e} & K'_e \\ 0 & 0 & 0 & 0 & A_{C2e}\Delta_2 & K'_e & -A_{C2e} - A_{0e} - K'_e \end{bmatrix} \begin{bmatrix} T_1 \\ T_2 \\ T_S \\ T_{C1} \\ T_{C2} \\ q_1 \\ q_2 \end{bmatrix}$$

$$= \begin{bmatrix} -3\sigma T^4(1-X_1)X_2 + A_{C1e}[q^*(T_{C1\text{old}}) - \Delta_1 T_{C1\text{old}}] - C_1 \\ -3\sigma T^4(1-X_2) + A_{C2e}[q^*(T_{C2\text{old}}) - \Delta_2 T_{C2\text{old}}] - C_2 \\ -3\sigma T^4 X_1 X_2 + A_{S1e}[q^*(T_{S\text{old}}) - \Delta_S T_{S\text{old}}] - C_S \\ 0 \\ -A_0 T \\ -A_{C1e}[q^*(T_{C1\text{old}}) - \Delta_1 T_{C1\text{old}}] - A_{S1e}[q^*(T_{S\text{old}}) - \Delta_S T_{S\text{old}}] \\ -A_{C2e}[q^*(T_{C2\text{old}}) - \Delta_2 T_{C2\text{old}}] - A_{0e}q \end{bmatrix} \tag{61}$$

where

$$Y \equiv 4\sigma T^3,$$

$$Y_i \equiv -2(1 - X_1)Y - A_{Ci} - A_{Cie}\Delta_i, \quad (i = 1, 2)$$

$$C_1 = S_{n1} + X_2(1 - X_1)L_a,$$

$$C_2 = S_{n2} + (1 - X_2)L_a,$$

and

$$C_S = S_{nS} + X_1X_2L_a - G.$$

The flow chart for the above calculation is shown in Fig. 7. It was found that two to six iterations were necessary in order to obtain a converged solution under usual conditions.

3. One-layer model (1LM)

For the one-layer model (1LM), the same physical processes are considered as those in the 2LM, as described in section 2. The equations to be solved are as follows:

- the heat-balance equation for the canopy layer

$$(1 - \alpha'_f)S_0 - S^{\downarrow}(h_1) + S^{\uparrow}(h_1) - S^{\uparrow}(h) + L_a - L^{\downarrow}(h_1) + L^{\uparrow}(h_1) - L^{\uparrow}(h) = H_C + lE_C. \tag{62}$$

- the heat-balance equation for the soil surface

$$S^{\downarrow}(h_1) - S^{\uparrow}(h_1) + L^{\downarrow}(h_1) - L^{\uparrow}(h_1) = H_S + lE_S + G \tag{63}$$

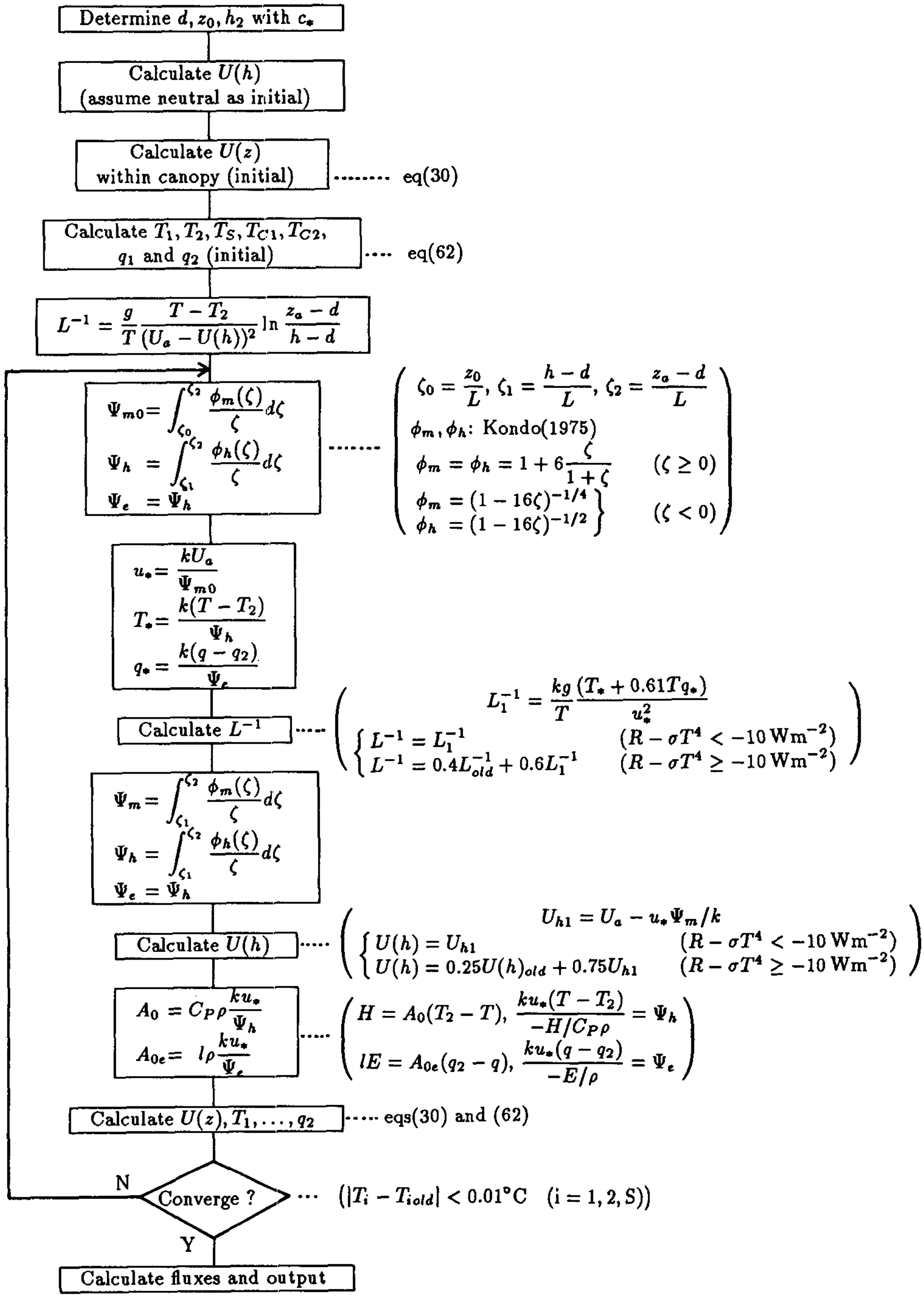

FIG. 7. Algorithm for the 2LM.

where

$$S^{\downarrow}(h_1) = (1 - \alpha_f')X_m S_0,$$

$$S^{\uparrow}(h_1) = (1 - \alpha_f')\alpha_S X_m S_0,$$

$$S^{\uparrow}(h) = (1 - \alpha_f')\alpha_S X_m X S_0,$$

$$X_m = \exp(-m\delta b),$$

$$X = \exp(-1.66\delta b),$$

$$\delta = h - h_1,$$

$$\alpha_f' \equiv (1 - X_m)\alpha_f,$$

$$L^{\downarrow}(h_1) = XL_a + (1 - X)\sigma T_C{}^4,$$

$$L^{\uparrow}(h_1) = \sigma T_S{}^4,$$

and

$$L^{\uparrow}(h) = X\sigma T_S^4 + (1 - X)\sigma T_C^4.$$

The expressions for the fluxes from the canopy elements to the surrounding air H_C and lE_C and the fluxes from the soil surface H_S and lE_S are similar to those in the 2LM.

- the continuity equations for the fluxes

$$H_C = H - H_S, \quad (64)$$

$$lE_C = lE - lE_S. \quad (65)$$

The fluxes H and lE are also the same as those in the 2LM and are given by Eqs. (25) and (26).

Since the canopy layer is not divided into two layers, it is not necessary to consider the diffusivity in the crown space [as expressed in Eq. (22)]. The representative height, z_1, similar to Eqs. (45) and (49), is given by

$$\left.\begin{aligned} z_1 &= \frac{h + h_1}{2}, & f < 0.5, \\ z_1 &= \frac{1}{\mu_0} \ln \frac{\exp(\mu_0 h) - \exp(\mu_0 h_1)}{\delta \mu_0}, & f \geq 0.5. \end{aligned}\right\} \quad (66)$$

Following Eqs. (62)–(65), the simultaneous simple equations can be reduced to four unknown variables, T_1, T_S, T_C, and q_1, and given as

$$\begin{bmatrix} A_C & (1-X)Y & Y_C & A_{Ce} \\ A_S & -Y - A_S - A_{Se}\Delta_S & (1-X)Y & A_{Se} \\ -A_C - A_0 - A_S & A_S & A_C & 0 \\ 0 & A_{Se}\Delta_S & A_{Ce}\Delta_C & -A_{Ce} - A_{0e} - A_{Se} \end{bmatrix} \begin{bmatrix} T_1 \\ T_S \\ T_C \\ q_1 \end{bmatrix} = \begin{bmatrix} -3\sigma T^4(1-X) + A_{Ce}[q^*(T_{C\text{old}}) - \Delta_C T_{C\text{old}}] - C_C \\ -3\sigma T^4 X + A_{Se}[q^*(T_{S\text{old}}) - \Delta_S T_{S\text{old}}] - C_S \\ -A_0 T \\ -A_{Ce}[q^*(T_{C\text{old}}) - \Delta_C T_{C\text{old}}] - A_{Se}[q^*(T_{S\text{old}}) - \Delta_S T_{S\text{old}}] - A_{0e} q \end{bmatrix} \quad (67)$$

where

$$Y \equiv 4\sigma T^3$$

$$Y_C \equiv -2(1-X)Y - A_C - A_{Ce}\Delta_C$$

$$C_C = (1 - \alpha_f')[1 - X_m + \alpha_S X_m(1 - X)]S_0 + (1 - X)L_a,$$

and

$$C_S = (1 - \alpha_f')(1 - \alpha_S)X_m S_0 + XL_a - G.$$

4. Observations and model application

The heat-balance components are calculated from data observed at a rice paddy field and an orchard and are then compared with the present model results.

a. Rice paddy field

Observations were conducted at Kitaura, in the northern part of Miyagi Prefecture, Japan. A horizontally homogeneous rice paddy field surrounds this observation site. Using cup anemometers and ventilated psychrometers, the profiles of wind, air temperature, and specific humidity were measured on a mast at six levels up to 10 m. Simultaneous observations of the downward solar and infrared radiation were made with a pyranometer and a pyrradiometer, while the radiative surface temperature was measured using an infrared-radiation thermometer (IRT) at 10 m above the rice paddy field (viewing nadir). The height of the rice plants and the leaf-area density were also measured. The height of the bottom of the crown space h_1 was assumed to be $0.15h$ for the rice field. The data (82 runs) were obtained during the period from 24 June to 20 August 1987 and from 26 May to 5 October 1988. The period of each run was 30 min (almost steady state in this period).

In this paper, the heat storage of the canopy and the energy used in the photosynthesis process are neglected. Thus, the heat flux into the soil layer G, one of the input parameters, can be estimated by

$$G = R_n - H - lE. \quad (68)$$

The fluxes H and lE are calculated from the observed profiles of wind speed, air temperature, and specific humidity above the canopy. From this point on, these values of the fluxes are called *observed values.* The net radiation R_n is written as

$$R_n = (1 - \alpha)S_0 + L_a - \sigma T_R^4, \quad (69)$$

where S_0 is the solar radiation, L_a the downward atmospheric infrared radiation, and T_R the radiative surface temperature. The albedo of the canopy α was calculated from Eq. (13) with $\alpha_f = 0.21$ and $\alpha_S = 0.08$, which were based on the albedo measurements on 12 July 1988. The value of α increases from 0.08 to 0.21 according to the growth of the rice.

Table 1 summarizes the observed values of the canopy height h, nondimensional canopy density c_*,

TABLE 1. Observed values of the canopy height h, canopy density c_*, the roughness z_0, the zero-plane displacement d, and the bulk transfer coefficients C_H and C_E. The data with values of $|T_R - T| < 1°C$ or $|H| < 5$ W m^{-2} were excluded when calculating C_H. Letter N is the number of data. The reference height for C_H and C_E is $10h$.

					C_H ($\times 10^{-3}$)			C_E ($\times 10^{-3}$)		
Period	h (m)	c_*	z_0 (m)	d (m)	Mean	Standard deviation	N	Mean	Standard deviation	N
1987										
24 June–26 July	0.35–0.70	0.66–1.4	0.029–0.081	0.23–0.50	3.9	1.4	4	3.1	0.5	6
7 August–20 August	0.85–0.96	1.6	0.086–0.11	0.52–0.68	7.9	1.0	4	3.9	0.7	7
1988										
26 May–11 June	0.07–0.18	0.023–0.10	0.0024–0.014	0–0.088	3.6	0.4	9	2.3	0.5	9
14 June–18 June	0.21–0.23	0.15–0.018	0.016–0.032	0–0.11	3.8	1.3	14	2.8	0.6	14
21 June–24 June	0.26–0.28	0.27–0.34	0.026–0.035	0.038–0.11	3.1	0.5	9	2.4	0.3	11
29 June–3 July	0.34–0.40	0.44–0.57	0.034–0.044	0.16–0.18	3.6	1.1	7	2.8	0.3	8
6 July–12 July	0.44–0.51	0.71–0.89	0.037–0.040	0.23–0.33	2.6	0.7	4	2.1	0.4	7
21 September–5 October	0.86	0.72–0.89	0.067–0.13	0.40–0.58	6.4	3.3	4	3.4	0.8	9

roughness z_0, zero-plane displacement d, and bulk transfer coefficients C_H and C_E. The bulk transfer coefficients given in the table, at a reference height of $10h$, are defined by the following equations:

$$H = C_P \rho C_H U_a (T_R - T), \tag{70}$$

$$lE = l\rho C_E U_a [q^*(T_R) - q]. \tag{71}$$

Variation can be seen in the values of C_H during some periods, which is partly due to an observation error and partly due to the inherent nature of bulk transfer coefficients discussed in section 6. The results of the zero-plane displacement and roughness length are also shown in Figs. 8 and 9 with model-calculated curves [Eqs. (39) and (43)].

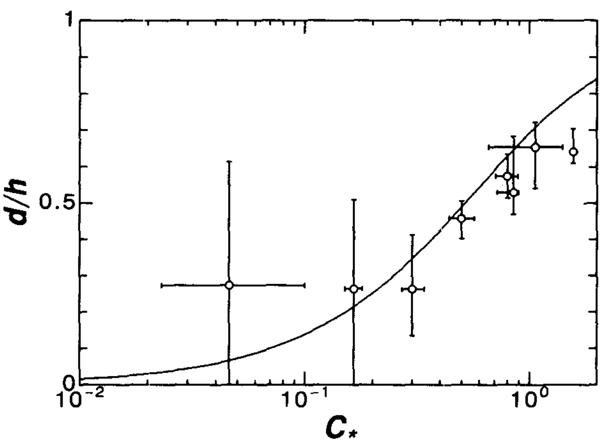

FIG. 8. Comparison of observed and calculated zero-plane displacement at the rice paddy field. Circles denote the mean values of each period in Table 1 and error bars denote the range minimum through maximum. The curve is model calculation [Eq. (39) with $h_1/h = 0.15$].

No data were obtained under very dry or hot conditions in the rice paddy field, so that Ω was specified as unity in Eq. (55) while j was given as a function of solar radiation and wind speed. The following values were adopted: $c_d = 0.18$, $c_h = 0.05$, and $\beta_S = 1$ (wet condition), where c_d is MLM tuning and c_h is experimentally determined (see Kondo and Watanabe 1991).

The two parameters for the stomatal resistance r_m and $S_{\rm abm}$ were determined so that the differences between the calculated and observed fluxes H and lE are minimal for a certain period. Most of the water vapor flux originates from water surfaces in May to early June, because the rice plants are small. Therefore, these data were not adequate to determine r_m and $S_{\rm abm}$. Moreover, the data from the period September–October are separated, because the rice plants are discolored, turning yellow, and the amount of evapotranspiration for this season changes (see Table 2). For fall

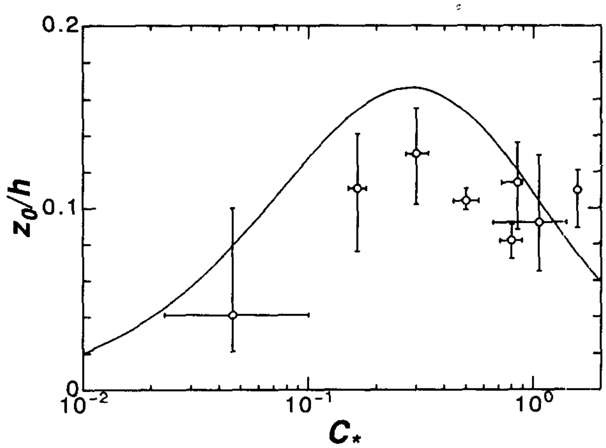

FIG. 9. Same as Fig. 9 but for roughness length. The curve is given by Eq. (43) with $h_1/h = 0.15$.

TABLE 2. Optimized values of r_m and S_{abm} for the rice paddy field.

Period	r_m (s m^{-1})	S_{abm} (W m^{-2})
Summer 1987 (24 June–20 August)	64	53
Summer 1988 (14 June–12 July)	31	289
Fall 1988 (21 September–5 October)	237	0
Summer 1987 and 1988 (14 June–20 August)	48	116

of 1988, $S_{abm} = 0$ and thus j does not depend on the solar radiation, which is consistent with the inactivity of plant physiology. In Fig. 10 the observed fluxes are compared with the values calculated by the 2LM with $r_m = 48$ s m^{-1} and $S_{abm} = 116$ W m^{-2}. Both of the fluxes are almost in agreement, within a range of ±20 W m^{-2}. Although Table 2 shows differences in r_m and S_{abm} between 1987 and 1988, they do not significantly affect the flux values (the difference between circles and squares in Fig. 10 are only about 20 W m^{-2}).

Figure 11 shows the relationship between j and S_{ab2}, where the various curves represent Eq. (55) for different values of U. The plotted values of j are obtained in order that the calculated and observed Bowen ratios agree for each run (henceforth j_{fit}). The j values increase with the decrease of wind speed (U, in the crown space) and with the increase of solar radiation. The values of j_{fit} almost coincide with the curves.

The relation between the saturation deficit $q^*(T_{C2}) - q_2$ and j is shown in Fig. 12; the ordinate indicates the difference between j_{fit} and j_{eq} [obtained from (55) with $\Omega = 1$]. No systematic dependence of j on the saturation deficit can be found. This supports the assumption that there is no influence of the saturation deficit in (55) (i.e., $\Omega = 1$).

b. Orchard

Similar heat-balance observations were made at an apple orchard located in Zinmachi, the central part of Yamagata Prefecture, Japan. Here a horizontally homogeneous orchard extends over 500 m on the windward side of the prevailing wind. The canopy height was measured at 4 m, with a trunk space of under 1 m. The leaf area density was measured as 0.5 m^2 m^{-3}. The profiles of wind speed, air temperature, and specific humidity above (up to 15 m) and within the canopy were observed with cup anemometers and ventilated psychrometers. The downward solar and infrared radiation was measured at a location outside of the canopy with a pyranometer and a pyrradiometer. Also, the solar radiation and reflection were measured at the forest floor. Average values of the canopy radiative temperature were measured from above, at a height of 7 m, by a moving IRT (see Fig. 13), while the radiative temperature of the leaves, trunk, and soil surface were measured using an IRT.

The heat flux into the soil layer was calculated from soil temperatures measured with thermocouples and bent-stem earth thermometers at depths of 0, 2, 4, 8, 15, 25, and 30 cm for three different locations. The values of the mass of soil-water content (measured by a weighing method) from the surface to 25 cm were in the range 0.3–0.5 for each day, and thus the soil surface was considered to be fully wet ($\beta_S = 1$; Kondo et al. 1990). The soil-water potential, measured with a tensiometer at the depth of 50 cm, ranged from −29 hPa to −44 hPa.

The observations were carried out over four days, 7, 8, 9, and 23 August 1988, resulting in seven runs of data being available. The period of each run was 30 min (almost steady state).

The results for each run are shown in Table 3. The reference height of C_H and C_E was 10 m, with the value of C_H being around 0.01 and C_E between 0.002 to 0.004. Examples of the profiles are shown in Fig. 14; the wind-speed profiles are logarithmic above 5 m. The drag coefficient of individual leaves c_d (=0.2) was determined so that the calculated wind speed in the upper canopy layer agreed with the observed speed. Thus, the nondimensional canopy density c_* was obtained as 0.4 for $h = 4$ m, and the corresponding zero-place displacement d was calculated as 1.66 m with $h_1 = 1$ m [see Eq. (39)]. The tower height of 15 m was too low to simultaneously determine d, z_0, H, and lE from profiles of the present observations. Accordingly, a calculated value of the zero-plane displacement ($d = 1.66$ m) was assumed to determine z_0, H, and lE [the value of z_0 from Eq. (43) with $d = 1.66$ m is 0.64 m].

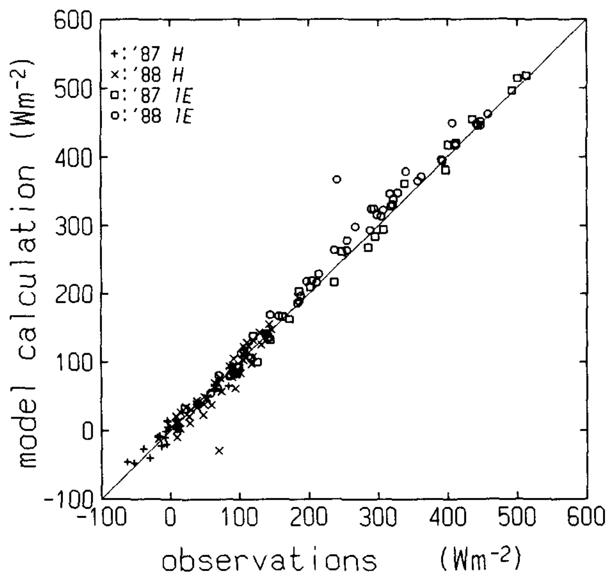

FIG. 10. Comparison of observed and calculated fluxes for the entire period except for the fall season at the rice paddy field. Calculated values are based on the 2LM with optimized parameters: $r_m = 48$ s m^{-1} and $S_{abm} = 116$ W m^{-2}.

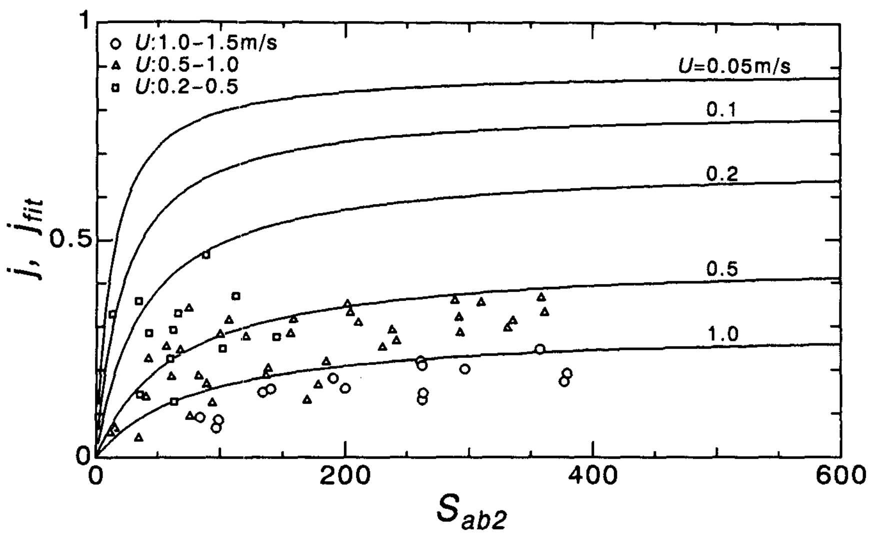

FIG. 11. The relation between the evapotranspiration factor of a leaf j and j_{fit} and the absorbed solar radiation in the $C2$ layer S_{ab2} during the summer season. The solid lines denote j [derived from Eq. (55) with $\Omega = 1$, $r_m = 48$ s m^{-1} and $S_{abm} = 116$ W m^{-2}], and the plotted points denote j_{fit}.

Using the observed albedo ($\alpha = 0.16$–0.18) and solar radiation at the forest floor, the two parameters of albedo were set at $\alpha_f = 0.24$ and $\alpha_S = 0.16$.

Equation (55) was used to determine the evapotranspiration factor j by assuming $\Omega = 1$. In the same manner as in the previous section, the two parameters of the stomatal resistance were determined: $r_m = 158$ s m^{-1} and $S_{abm} = 0$ (for $c_h = 0.05$). Thus, j is a function of only wind speed, and therefore independent of solar radiation. As the saturation deficit increases, j_{fit} slightly decreases, unlike the case for the rice paddy field.

Figure 15 displays a scatter diagram of observed fluxes based on the profile method versus calculated values by the 2LM, using optimum values of r_m and S_{abm}. The scatter of the fluxes is larger than that for the rice paddy field (Fig. 10), which may be partly ascribed to the inaccuracies that occur in the observed fluxes.

5. Comparison among the one-layer, two-layer, and multilayer models

In section 4 it was found that the 2LM agreed well with the observed heat balance for a rice paddy field and an orchard. In this section several results from

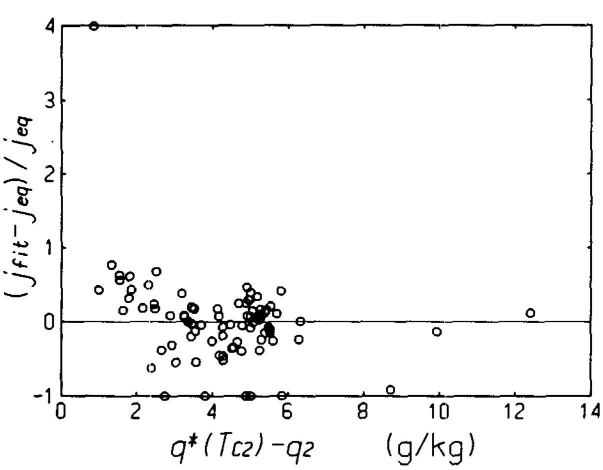

FIG. 12. Normalized difference between j_{fit} and j_{eq} versus saturation deficit.

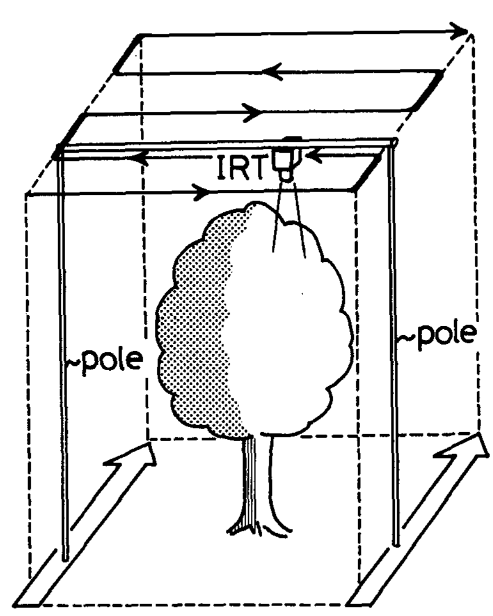

FIG. 13. Schematic illustration of the measurement of the canopy radiative temperature with a moving infrared-radiation thermometer (IRT).

TABLE 3. Results of the orchard observations. Variable T_R is the canopy radiative temperature measured at the height of 7 m. The bulk transfer coefficients C_H and C_E are defined by Eqs. (70) and (71). The unit for the flux is watts per square meter. The reference height of C_H and C_E is 10 m. Parenthesized data indicate that the temperature difference is less than 0.05°C.

Date	Run number	z_0 (m)	S_0	H	lE	G	Residual	U_a (m s^{-1})	T (°C)	q (g kg^{-1})	T_R (°C)	C_H (×10^{-3})	C_E (×10^{-3})
7	1	0.307	363	10	185	23	48	2.40	29.40	17.2	30.0	6.0	2.9
8	1	0.564	644	48	315	54	48	4.12	30.30	16.8	33.8	2.9	1.6
8	2	0.613	454	6	189	16	128	4.00	30.15	17.1	31.2	1.2	1.5
9	1	0.400	713	95	390	113	−69	1.46	30.60	15.8	35.0	12.9	4.8
9	2	0.494	532	121	459	1	−179	3.67	30.60	16.8	32.2	17.9	3.3
23	1	0.493	489	8	361	48	−29	3.60	29.80	18.9	31.1	1.5	3.7
23	2	0.584	224	−11	234	−12	−38	4.35	28.75	18.4	28.7	(44.0)	3.1

three canopy models, 1LM (section 3), 2LM, and MLM, are compared under the following conditions.

$$S_0 = 600, 0 \text{ W m}^{-2}$$
$$L_a = 319 \text{ W m}^{-2}$$
$$U_a = 5 \text{ m s}^{-1}$$
$$T = 20°\text{C}$$
$$q = 10 \text{ g kg}^{-1}$$
$$h = 1 \text{ m}$$
$$h_1 = 0.5 \text{ m}$$
$$c_d = 0.1$$
$$c_h = 0.05$$
$$c_e = 0.01$$
$$b = a$$
$$\alpha_f = \alpha_S = 0$$

Figure 16 presents examples of calculated sensible heat fluxes using the 1LM, 2LM, and MLM versus the canopy density. Since the MLM does not consider atmospheric stability, the 1LM and 2LM are used under neutral conditions for the purpose of comparison. These figures suggest that the 1LM is sufficient for the estimation of fluxes, since the difference in the flux is within several watts per square meter for dense canopies under conditions of large-incident solar radiation (600 W m^{-2}). The 2LM gives the same fluxes as those by the MLM within an error of about 5 W m^{-2}.

When the leaf-area density varies vertically or the leaves are localized in the upper or lower part of a canopy, the 1LM or 2LM may not yield correct fluxes. Sellers et al. (1989) have introduced the height of maximum canopy density in order to deal with such a leaf area distribution. However, this problem may be overcome by using values of h, h_1, and a for the individual leaf-area distribution.

6. Discussion

a. Nonequilibrium soil layer

In most cases, due to its large heat capacity, a soil layer is not thermally in equilibrium ($G \neq 0$) under varying external conditions (e.g., incident radiation, air temperature). The melting of a snow surface is also not in an equilibrium state, since T_S cannot exceed 0°C until the snow completely vanishes. In this section, the nonequilibrium situation is discussed by fixing T_S compulsorily at an arbitrary value, which differs from that for the steady state.

The conditions of the calculation are as follows:

$$S_0 = 400 \text{ W m}^{-2},$$
$$L_a = 215 \text{ W m}^{-2},$$
$$U_a = 5 \text{ m s}^{-1},$$
$$T = 0°\text{C}$$

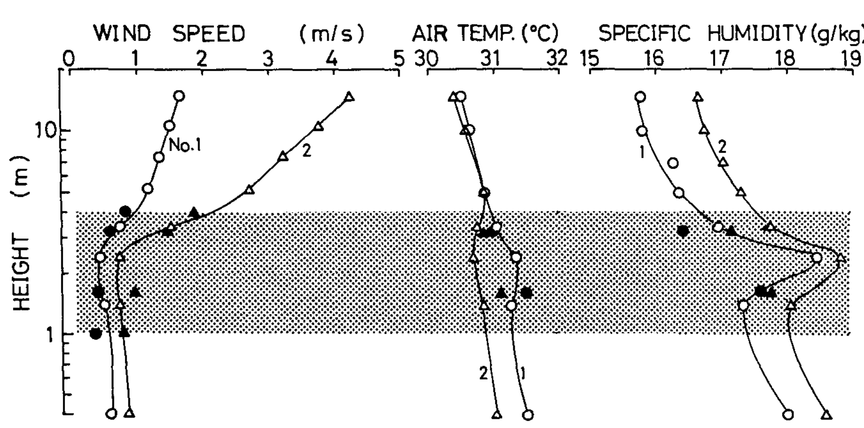

FIG. 14. Examples of the wind, air temperature, and specific-humidity profiles at the orchard for 9 August 1988. Labeled number corresponds to run number in Table 3. Open circles: observed data. Closed circles: 2LM. Stippled area denotes the crown space.

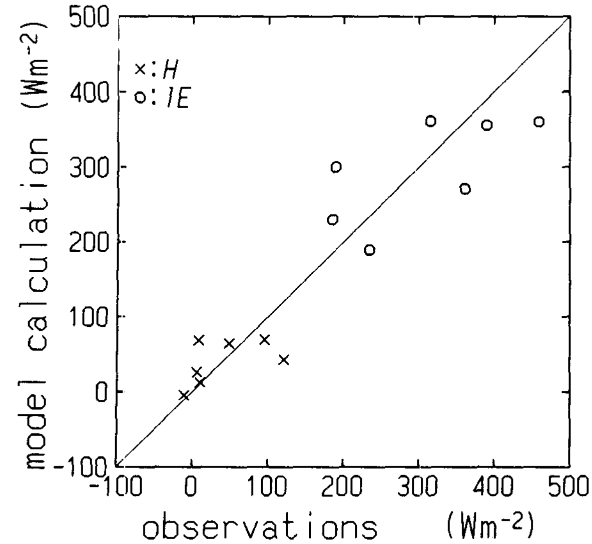

FIG. 15. Comparison of observed and calculated fluxes for the orchard. Calculated values are from the 2LM with the optimized parameters: $r_m = 158 \text{ s m}^{-1}$ and $S_{abm} = 0$.

and

$$q = 2.6 \text{ g kg}^{-1}.$$

The canopy parameters are the same as those in section 5, and only the cases of $\alpha_s = 0$ and $\alpha_s = 0.6$ are examined. For reference, the bulk transfer coefficients for the steady state ($G = 0$) obtained by the 2LM are shown in Fig. 17.

The abscissa of Fig. 18 indicates the fixed value of T_S, and the ordinate the bulk transfer coefficient C_H defined by Eq. (70), where H has been calculated by the 2LM. When $T_S < T = 0°C$, negative values of C_H are encountered. Figure 19 shows such a situation: since the crown space is heated by solar radiation, the sensible heat is transferred from the canopy layer to the atmosphere ($H > 0$). However, T_R is affected by T_S (fixed lower than T) and $T_R < T$ occurs, resulting in a negative C_H. At night, on the other hand, since the crown space is cooled, $H < 0$ and $T_R - T > 0$, and thus $C_H < 0$ occurs again.

Therefore, the bulk transfer coefficient C_H may change with T_S as well as with the canopy structure. Figure 20 shows a T_S dependency of sensible heat fluxes calculated by the bulk formula given in (70) using two different values of C_H. The solid lines correspond to the C_H value obtained by the above method, while the broken lines to that obtained by assuming a steady state ($G = 0$). In both methods, the same value of $T_R - T$, which was calculated by the 2LM with a fixed T_S, is used. Figure 20a gives results of the calculations for $\alpha_f = \alpha_S = 0$, and Fig. 20b for $\alpha_S = 0.6$ (old snow). The solid and broken lines for each c_* intersect each other at a certain value of T_S, where the steady state should be achieved. The inclinations of the broken lines are greater than those of the solid lines for $c_* = 0.1$ and 0.3. This means that values of H obtained with C_H for the steady state are greater than the actual H when T_S is higher than the steady-state value, and vice

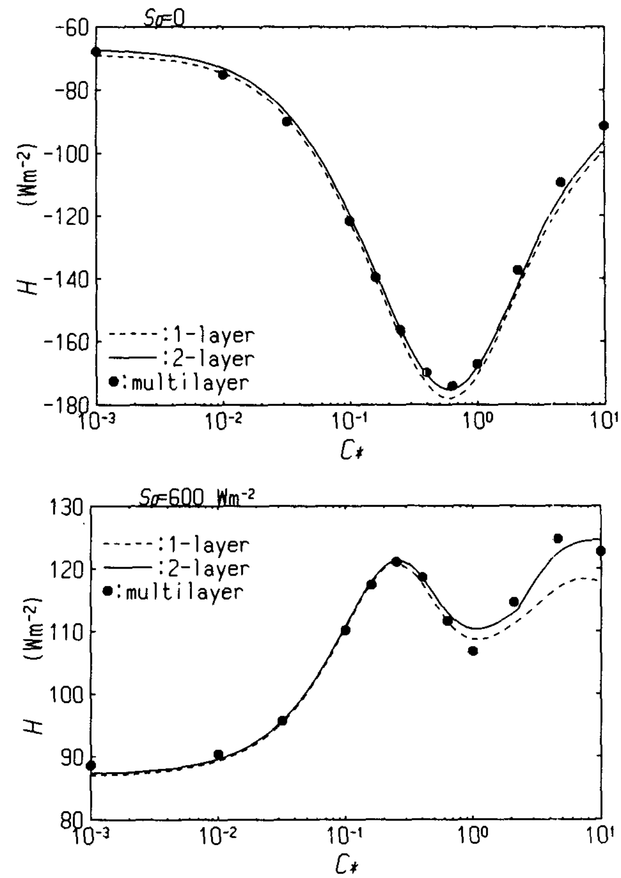

FIG. 16. Examples of calculated sensible heat fluxes using the 1LM, 2LM, and MLM vs canopy density for (a) $S_0 = 0$ and (b) $S_0 = 600$ W m^{-2}.

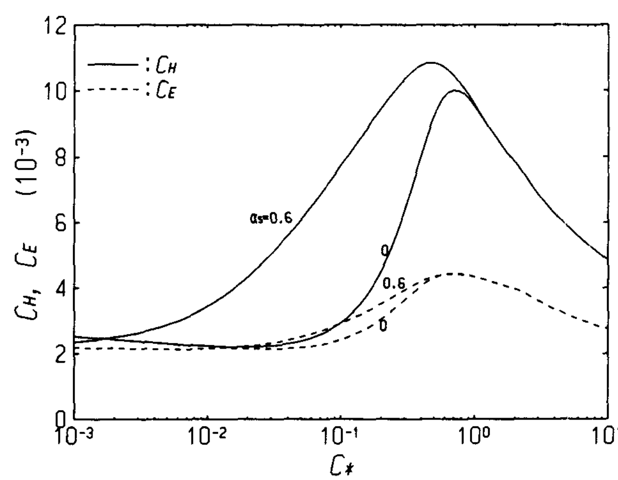

FIG. 17. Calculated values of the bulk coefficients in the steady state by use of the 2LM as a function of canopy density, having a parameter of α_S.

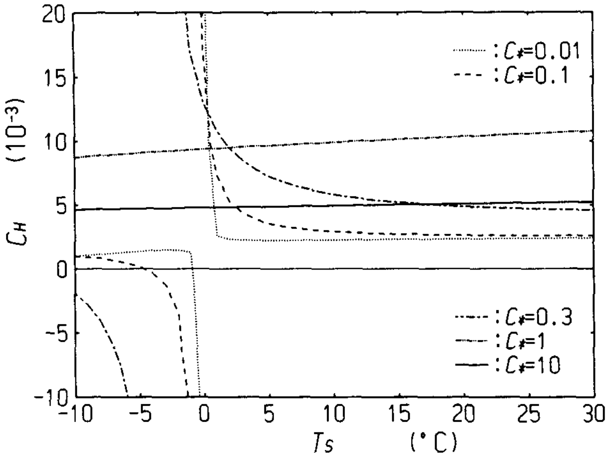

FIG. 18. The variation of the bulk coefficient C_H when the fixed soil surface temperature is used for various values of canopy density, c_*, with $\alpha_S = 0$.

versa when T_S is lower. This tendency is more significant in Fig. 20b ($\alpha_S = 0.6$) because the reflected solar radiation from the ground also heats the crown space.

These errors result from the fact that the temperature of the canopy elements, where the most part of the sensible heat is exchanged, differs greatly from T_R. A value of T_R is not representative of the temperature of the crown space and is influenced by T_S. It is easy to measure T_R with an infrared-radiation thermometer

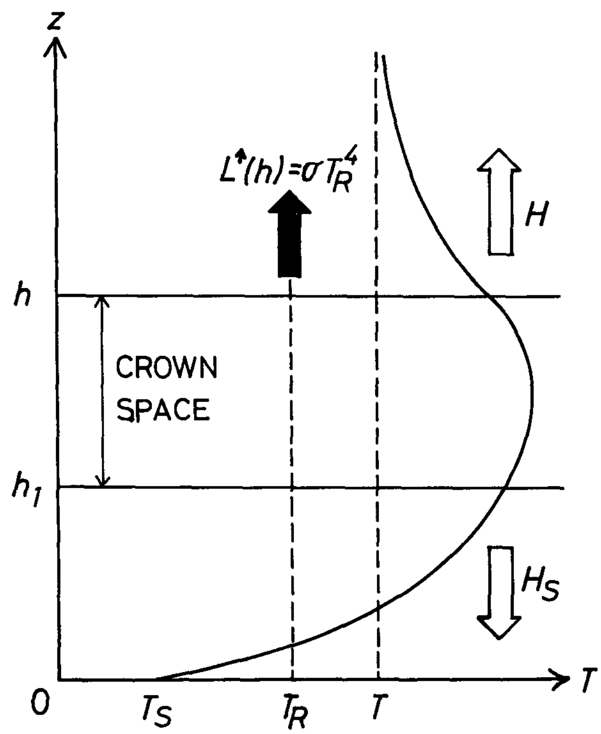

FIG. 19. An example of an air temperature profile when $C_H < 0$.

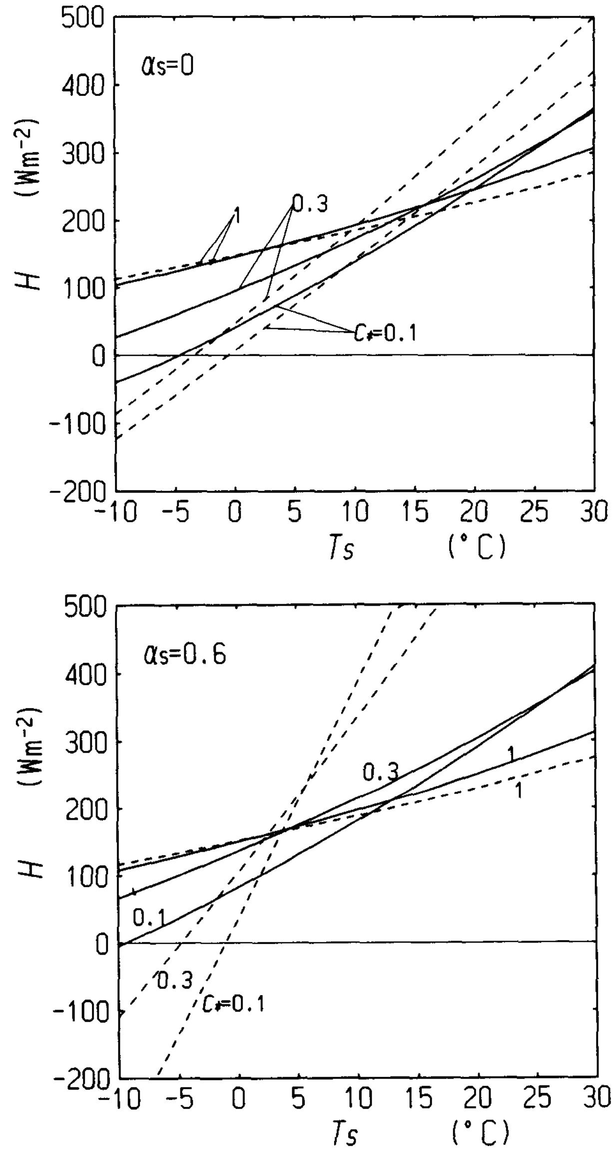

FIG. 20. The variation of the sensible heat flux with a fixed soil surface temperature for (a) $\alpha_S = 0$ and (b) $\alpha_S = 0.6$. Solid lines: using the 2LM with fixed T_S. Broken lines: with C_H (steady state) and $T_R - T$.

from above, but the estimated sensible heat flux is erroneous if the soil layer is not in an equilibrium state.

This relationship is similar to that between latent heat lE and C_E. Moreover, C_H and C_E also depend on external conditions, such as incident radiation or wind speed. These problems are discussed in Kondo and Watanabe (1992).

b. Dependence of radiative ground-surface temperature on the viewing angle

The radiative ground-surface temperature depends on the viewing angle and is written using the 2LM as

$$T_R(\theta)^4 = (1 - X_{m1})X_{m2}T_{C1}^4 + (1 - X_{m2})T_{C2}^4 + X_{m1}X_{m2}T_S^4, \quad (72)$$

where θ is viewing nadir angle and X_{mi} is defined by Eq. (11). If T_R is measured from three or more different viewing angles (e.g., by an infrared sensor on a satellite with an in-track tilt capability), it is basically possible to obtain T_{C1}, T_{C2}, and T_S using (72).

Huband and Monteith (1986) showed that the radiative surface temperature measured at an angle of 55° to the vertical was well related to the air temperature at the height of $z_0 + d$ in a wheat canopy. The best viewing angle to estimate sensible and latent heat fluxes for the surface temperature of bulk formulas probably exists. However, it depends on canopy density and other conditions. A more detailed discussion will be given in the future.

7. Concluding remarks

A simple heat-balance model with either one or two layers in the canopy has been developed. This model can easily determine the roughness length and the zero-plane displacement of a vegetated surface if the canopy information (canopy density, canopy height, and canopy-layer thickness) is available, while also calculating the heat balance of the canopy. The heat-balance components obtained by this model are, for the most part, in agreement with those calculated by use of a multilayer model for usual leaf-area distributions. Moreover, the proposed model yields almost the same sensible and latent heat fluxes above the canopies as observed for a rice paddy field and an orchard.

The two-layer model achieves better results when the radiative ground temperature measured from space has a dependency on the viewing angle (for this case, it is necessary to know the air temperature profile in the canopy). On the other hand, the one-layer model is sufficient, if the requirements are only the steady fluxes between the vegetated surface and the atmosphere.

Application of this model to non-steady-state problems can be achieved by including the canopy heat capacity. The present model has been joined to soil-layer models and snow-cover models. The results of such joint models will be discussed elsewhere.

Acknowledgments. The authors wish to thank R. Kimura and R. Yahagi for their cooperation during the observations. They also would like to thank their colleagues at Tohoku University for assistance in the observations and for valuable comments.

APPENDIX

List of Symbols

Subscript i denotes each canopy layer $C1$ and $C2$ ($i = 1, 2$):

- a leaf-area density (one-sided)
- $A_0 = C_P\rho k u_* / \Psi_h$
- $A_{0e} = l\rho k u_* / \Psi_e$
- $A_{Ci} = C_P\rho c_h a\delta_i U(z_i)$
- $A_{Cie} = l\rho c_{ei} a\delta_i$
- $A_S = C_P\rho C_{HS} U(h_1)$
- $A_S e = l\rho\beta C_{HS} U(h_1)$
- b extinction coefficient
- c_d drag coefficient of individual leaves
- c_e, c_h transfer coefficients of individual leaves for latent and sensible heat
- c_* nondimensional canopy density ($= c_d a h$)
- c_{*1} variable for the wind profile, a function of c_*
- C_E, C_H bulk transfer coefficients above the canopy for latent and sensible heat
- C_{HS} bulk transfer coefficient of a soil surface for sensible heat
- C_P specific heat of air
- d zero-plane displacement
- E water vapor flux from the canopy layer to the air above the canopy
- E_{12} water vapor flux from the $C1$ layer to the $C2$ layer
- E_C water vapor flux from the canopy elements to the surrounding air (1LM)
- E_{Ci} same as E_C but for each canopy layer (2LM)
- E_S water vapor flux from the soil surface
- f partition coefficient for the wind profile, a function of c_*
- G heat flux into the soil layer
- h canopy height
- h_i height of the bottom of each canopy layer
- H sensible heat flux from the canopy layer to the air above the canopy
- H_{12} sensible heat flux from the $C1$ layer to the $C2$ layer
- H_C sensible heat flux from the canopy elements to the surrounding air (1LM)
- H_{Ci} same as H_C but for each canopy layer (2LM)
- H_S sensible heat flux from the soil surface
- j evapotranspiration factor of a leaf ($= c_e/c_h$)
- j_i evapotranspiration factor of a leaf for each canopy layer
- j_{fit} optimized evapotranspiration factor of a leaf
- k von Kármán constant
- K_E, K_H eddy diffusivity for latent and sensible heat transfer
- $K' = C_P\rho K_H(h_2)/(z_1 - z_2)$
- $K'_e = l\rho K_E(h_2)/(z_1 - z_2)$
- l latent heat of evaporation
- L Monin–Obukhov length
- $L^\downarrow$, $L^\uparrow$ downward and upward flux of longwave radiation
- L_a downward flux of atmospheric radiation

L_{ni} net longwave radiation absorbed by each canopy layer
L_{nS} net longwave radiation absorbed by the soil layer
$m = \sec\theta$
q specific humidity at the reference height z_a
q_i specific humidity in each canopy layer
q^* saturation specific humidity
r_a aerodynamic resistance for a leaf surface
r_s stomatal resistance
r_m minimum stomatal resistance
R_n net radiation above the canopy
$S^\downarrow, S^\uparrow$ downward and upward flux of shortwave radiation
S_0 incident flux of solar radiation
S_{ab} shortwave radiation absorbed by a unit leaf area
S_{abm} S_{ab} when $r_s = 2r_m$
S_{ni} net shortwave radiation absorbed by each canopy layer
S_{nS} net shortwave radiation absorbed by the soil layer
T air temperature at the reference height z_a
T_i air temperature in each canopy layer
T_C leaf surface temperature (1LM)
T_{Ci} leaf surface temperature in each canopy layer (2LM)
T_R radiative surface temperature measured from above the canopy
T_S soil surface temperature
u_* friction velocity above the canopy
u_{*s} friction velocity in the trunk space
U wind speed
U_a wind speed at the reference height z_a
x $= \log c_*$
X transmittance of the canopy layer for longwave and reflected shortwave radiation (1LM)
X_i same as X but for each canopy layer (2LM)
X_m same as X but for direct solar radiation (1LM)
X_{mi} same as X_m but for each canopy layer (2LM)
z height above the soil surface
z_0 roughness length above the canopy
z_{0S} roughness length of the soil surface
z_a reference height (above the canopy)
z_i representative height of each canopy layer
α albedo above the canopy
α_f leaf reflectance at the canopy top
$\alpha_f' = (1 - X_m)\alpha_f(1\text{LM});$
$\quad = (1 - X_{m1}X_{m2})\alpha_f(2\text{LM})$
α_S reflectance of the soil surface
β_S moisture availability of the soil surface
δ thickness of the crown space (1LM)
δ_i thickness of each canopy layer (2LM)
$\Delta_C = dq^*/dT\,(T = T_{C\text{old}})$
$\Delta_i = dq^*/dT\,(T = T_{Ci\text{old}})$
$\Delta_S = dq^*/dT\,(T = T_{S\text{old}})$
$\zeta = z/L$
θ solar zenith angle or viewing nadir angle
Λ mixing length
$\mu = c_d a/(2k^2)$
ρ air density
σ Stefan–Boltzmann constant
ϕ_h, ϕ_m nondimensional temperature gradient and wind shear
$\Psi_e, \Psi_h, \Psi_m = \int (\phi/\zeta)d\zeta$
Ω correction factor of r_s

REFERENCES

Deardorff, J. W., 1978: Efficient prediction of ground surface temperature and moisture, with inclusion of a layer of vegetation. *J. Geophys. Res.*, **83**, 1889–1903.

Dickinson, R. E., 1984: Modeling evapotranspiration for three-dimensional global climate models. *Climate Processes and Climate Sensitivity, Geophys. Monogr.*, No. 29, Amer. Geophys. Union, 58–72.

Huband, N. D. S., and J. L. Monteith, 1986: Radiative surface temperature and energy balance of a wheat canopy. I: Comparison of radiative and aerodynamic canopy temperature. *Bound.-Layer Meteor.*, **36**, 107–116.

Inoue, E., 1963: On the turbulent structure of airflow within crop canopies. *J. Meteor. Soc. Japan.*, **41**, 317–326.

Inoue, K., T. Sakuratani, and Z. Uchijima, 1984: Stomatal resistance of rice leaves as influenced by radiation intensity and air humidity. *J. Agric. Meteorol. (Tokyo)*, **40**, 235–242.

Kondo, J., 1975: Air-sea bulk transfer coefficients in diabatic conditions. *Bound.-Layer Meteor.*, **9**, 91–112.

——, and S. Akashi, 1976: Numerical studies on the two-dimensional flow in horizontally homogeneous canopy layers. *Bound.-Layer Meteor.*, **10**, 255–272.

——, and A. Kawanaka, 1986: Numerical study on the bulk heat transfer coefficient for a variety of vegetation types and densities. *Bound.-Layer Meteor.*, **37**, 285–296.

——, and T. Yamazaki, 1990: A prediction model for snowmelt, snow surface temperature, and freezing depth using a heat balance method. *J. Appl. Meteor.*, **29**, 375–384.

——, and T. Watanabe, 1992: Studies on the bulk transfer coefficients over vegetated surface with the multilayer energy budget model. *J. Atmos. Sci.*, **49**, in press.

——, N. Saigusa, and T. Sato, 1990: A parameterization of evaporation from bare soil surfaces. *J. Appl. Meteor.*, **29**, 385–389.

Sellers, P. J., Y. Mintz, Y. C. Sud, and A. Dalcher, 1986: A simple biosphere model (SiB) for use within general circulation models. *J. Atmos. Sci.*, **43**, 505–531.

——, J. W. Shuttleworth, J. L. Dorman, A. Dalcher, and J. M. Roberts, 1989: Calibrating the simple biosphere model for Amazonian tropical forest using field and remote sensing data. Part I: Average calibration with field data. *J. Appl. Meteor.*, **28**, 727–759.

van de Griend, A. A., and J. H. van Boxel, 1989: Water and surface energy balance model with a multilayer canopy representation for remote sensing purposes. *Water Resour. Res.*, **25**, 949–971.

Watanabe, T., and J. Kondo, 1990: The influence of canopy structure and density upon the mixing length within and above vegetation. *J. Meteor. Soc. Japan*, **68**, 227–235.